J Plant Growth Regul
DOI 10.1007/s00344-015-9553-2

A Forward Genetic Screen for New Regulators of Auxin-mediated Degradation of Auxin Transport Proteins in *Arabidopsis thaliana*

Radka Zemová[1] · Marta Zwiewka[1] · Agnieszka Bielach[1] · Hélène S. Robert[1] · Jiří Friml[2]

Received: 18 June 2015 / Accepted: 10 September 2015

Abstract The plant hormone auxin (indole-3-acetic acid) is a major regulator of plant growth and development including embryo and root patterning, lateral organ formation and growth responses to environmental stimuli. Auxin is directionally transported from cell to cell by the action of specific auxin influx [AUXIN-RESISTANT1 (AUX1)] and efflux [PIN-FORMED (PIN)] transport regulators, whose polar, subcellular localizations are aligned with the direction of the auxin flow. Auxin itself regulates its own transport by modulation of the expression and subcellular localization of the auxin transporters. Increased auxin levels promote the transcription of *PIN2* and *AUX1* genes as well as stabilize PIN proteins at the plasma membrane, whereas prolonged auxin exposure increases the turnover of PIN proteins and their degradation in the vacuole. In this study, we applied a forward genetics approach, to identify molecular components playing a role in the auxin-mediated degradation. We generated EMS-mutagenized *Arabidopsis PIN2*::*PIN2:GFP*, *AUX1*::*AUX1:YFP eir1 aux1* populations and designed a screen for mutants with persistently strong fluorescent signals of the tagged PIN2 and AUX1 after prolonged treatment with the synthetic auxin 2,4-dichlorophenoxyacetic acid (2,4-D). This approach yielded novel *auxin degradation* mutants defective in trafficking and degradation of PIN2 and AUX1 proteins and established a role for auxin-mediated degradation in plant development.

Keywords Root development · Polar auxin transport · Plasma membrane · AUX1 · PIN2 · Vacuolar degradation

Introduction

Eukaryotic cells present at the cell surface a specific set of plasma membrane proteins that modulate responses to internal and external cues and whose activity is often regulated by protein degradation (Kleine-Vehn and others 2008). Cell polarity is one of the fundamental properties of multicellular organisms and is tightly linked with processes such as cell division, differentiation, cellular signalling and intercellular communication. The signalling molecule, auxin, has been linked to multiple aspects of plant development including coordinated cell and tissue polarization. The distribution of auxin depends largely on its directional transport from cell to cell (Adamowski and Friml 2015). The chemiosmotic model of auxin transport predicted the asymmetric localization of auxin efflux carriers at one side of the transporting cells as a determining feature for the directionality of the auxin movement within the field of cells. This insight was confirmed experimentally (Wiśniewska and others 2006) and connects polarities at the cellular and tissue levels (Feraru and Friml 2008; Sauer and others 2006). By a forward genetic approach, the plasma membrane-resident transporters of the auxin transport have been identified such as PIN-FORMED (PIN) auxin export

Electronic supplementary material The online version of this article (doi:10.1007/s00344-015-9553-2) contains supplementary material, which is available to authorized users.

✉ Jiří Friml
jiri.friml@ist.ac.at

[1] Mendel Centre for Genomics and Proteomics of Plant Systems, CEITEC MU – Central European Institute of Technology, Masaryk University, 625 00 Brno, Czech Republic

[2] Institute of Science and Technology Austria (IST Austria), 3400 Klosterneuburg, Austria

Journal : Large 344 | Dispatch : 5-11-2015 | Pages : 12
Article No. : 9553 | ☐ LE | ☐ TYPESET
MS Code : JPGR-15-0235 | ✔ CP | ✔ DISK

and AUXIN-RESISTANT 1 (AUX1) auxin import proteins (Bennett and others 1996; Luschnig and others 1998; Petrášek and others 2006).

In *Arabidopsis*, *AUX1* is expressed in the root tips in the protophloem, columella, epidermal cells and lateral root caps (Swarup and others 2001), whereas *PIN2* is expressed in epidermal and cortical cells (Kleine-Vehn and others 2008). Together, these proteins are required for root growth, in particular in gravitropic response, and their abundance is tightly regulated at multiple levels including a feedback regulation by auxin itself. Short auxin treatments ($\leqslant$2 h) activate the transcription of different *PIN* genes (Vieten and others 2005) and can stabilize PIN at the plasma membrane by inhibiting clathrin-mediated internalization (Paciorek and others 2005; Robert and others 2010). In contrast, prolonged auxin treatment also induces the turnover of PIN proteins by promoting their vacuolar trafficking (Abas and others 2006; Sieberer and others 2000). Similar to auxin, light plays an important role in vacuolar degradation of PIN2 and other PIN proteins. In the absence of light, steady-state levels of PIN2 at the plasma membrane are greatly reduced, and a large part of PIN2 is removed from the plasma membrane to the vacuoles (Laxmi and others 2008).

The vacuolar trafficking pathway is used by multiple cargo proteins including auxin transporters for their degradation (Kleine-Vehn and others 2008; Löfke and others 2013; Marhavy and others 2011). Vacuoles are crucial organelles in plant cells, playing important roles in plant physiology and development. They can be divided into two main groups: (1) lytic vacuoles that, similarly to the lysosomes found in animals, perform a general degradation, (2) protein storage vacuoles that mainly store reserve proteins in seeds. Besides the general degradation function, lytic vacuoles are very important for breakdown of storage proteins during seed germination, thus providing the germinating seedlings with the necessary nutrients (Feraru and others 2010). The rough contours of the vacuolar trafficking pathways have been characterized, and the recent forward genetic screens using fluorescently tagged PIN proteins further contributed to identification of the molecular components of this process (Feraru and others 2010; Nodzynski and others 2013; Zwiewka and others 2011). Identification of other components of PIN trafficking using similar forward genetic approaches (Feraru and others 2010; Tanaka and others 2009; Tanaka and others 2013; Tanaka and others 2014) demonstrated the viability of this approach. Here we performed a screen using mutagenized *PIN2*::*PIN2:GFP AUX1*::*AUX1:YFP eir1 aux1* population and identified and characterized new *auxin degradation* (*ade*) mutants specifically affecting auxin-dependent PIN2 and/or AUX1 plasma membrane turnover.

Materials and Methods

EMS Mutagenesis and Mutant Screen

The EMS mutagenesis was performed on seeds of transgenic *Arabidopsis thaliana* plants (ecotype Col-0) harbouring *PIN2*::*PIN2:GFP AUX1*::*AUX1:YFP* transgenes in the *aux1 eir1-1* mutant background, obtained by crossing previously described lines: *AUX1*::*AUX1:YFP*, *aux1* (Bennett and others 1996), *PIN2*::*PIN2:GFP* (Xu and Scheres 2005) and *pin2/eir1-1* (Luschnig and others 1998).

Seeds were soaked in 0.2 % EMS solution for 8 h and sown on soil. Five M1 plants were pooled and M2 seeds were bulk harvested. From each pool, 200 to 250 of 5-day-old seedlings were used for screening. Overall of 61,400 M2 seedlings from 307 independent pools, descended from approximately 1500 M1 plants, were grown for 4 days on solid 0.5× Murashige and Skoog (MS) medium (as described below) and transferred on new plates supplemented with 1 µM 2,4-D (Sigma) for 20 h. Seedlings were analysed under a fluorescence stereomicroscope and screened for an elevated fluorescence signal of PIN2:GFP or AUX1:YFP as compared with the 2,4-D treated parental *PIN2*::*PIN2:GFP AUX1*::*AUX1:YFP aux1 eir1-1* line as control. After re-screening, the phenotype was confirmed for 12 mutants that, in the next generation, showed a consistent and reliable cellular phenotype. Three lines exhibited specifically resistance to 2,4-D, and they were designed as *ade1* to *ade3*.

Plant Material and Growth Conditions

For all experiments, the parental *PIN2*::*PIN2:GFP AUX1*::*AUX1:YFP aux1 eir1-1* line is used as control. The identified *ade* mutants were backcrossed into the parental *PIN2*::*PIN2:GFP AUX1*::*AUX1:YFP aux1 eir1-1* line. F1 plants were self-pollinated, yielding a polymorphic F2 population. All *ade* mutant lines are recessive for the mutation of interest, which segregates at 25 % (*ade1* $n = 58$ mutants out of 235, *ade2* $n = 54/215$, *ade3* $n = 42/170$) in F2 after outcross. From this generation, the individuals showing an increased fluorescent signal of both PIN2-GFP and AUX1-YFP after treatment with 1 µM 2,4-D were selected. The seeds of homozygous F3 population and following generations at the comparable age of each genotype were used for the phenotype analysis. Surface-sterilized seeds were sown on 0.5× MS medium containing 0.8 % plant agar (Duchefa) supplemented with 1 % sucrose (Penta) (pH 5.8) and vernalized for 3 days in the dark at 4 °C. The seedlings were grown on vertically oriented plates at 18 °C and were illuminated by 150 µmol/s m^2 light intensity, in 16-h light and 8-h dark photoperiod

Journal : Large 344 | Dispatch : 5-11-2015 | Pages : 12
Article No. : 9553 | LE | TYPESET
MS Code : JPGR-15-0235 | CP | DISK

cycles (referred to as long day, LD) for 5 days in a phytotron.

Treatment with Auxins and Microscopy

For the screen, 4-day-old seedlings were incubated in 1 μM 2,4-D (Sigma) dissolved in DMSO (Sigma) and diluted in solid 0.5× MS medium, for 20 h. For phenotyping analysis, 5-day-old seedlings were grown on solid media supplemented with 10 nM 2,4-D and 20 nM NAA (Sigma) for 5 days. For PIN2-GFP signal intensity measurements, 5-day-old seedlings were grown on solid media supplemented with 20 nM NAA for 3 h. The selection of mutant lines was done with Olympus SZX16 stereomicroscope equipped with SZX2 fluorescence unit and DP73 camera, under ×1.6 magnification. For the cotyledon venation pattern analysis, the stereomicroscopy was used with dark filed illumination. For lateral root analysis, an Olympus BX61 microscope equipped with a DP70 CCD camera using a 40× DIC objective with water immersion was used. For live cell imaging of GFP and YFP signals, seedling roots were mounted in liquid 0.5× MS medium. Confocal images were done with a Zeiss LSM 780 confocal microscope using a ×40 objective with water immersion.

Root and Hypocotyl Phenotype Analysis

Detailed phenotype analysis was carried out on the backcrossed, homozygous mutant lines. The seedlings were growing on auxin from the beginning. Root length measurements were performed on 5-day-old seedlings grown at 22 °C. For the hypocotyl length assay, vernalized seeds were illuminated by 150 μmol/s m^2 light for 5 h, wrapped by double aluminium foil and kept vertically for 4 days at 22 °C. Lateral root density analysis was accomplished using the control line and *ade3* mutants, because only this mutant line showed obvious lateral root phenotype by the naked eye. Seedlings were grown vertically on solid 0.5× MS medium alone and solid 0.5× MS medium supplemented with 10 nM 2,4-D for 8 days in a LD photoperiod at 22 °C. The seedlings were placed overnight in 70 % EtOH to remove chlorophyll and cleared accordingly to the protocol described in Malamy and Benfey (1997). Lateral root density was defined as the number of emerged lateral

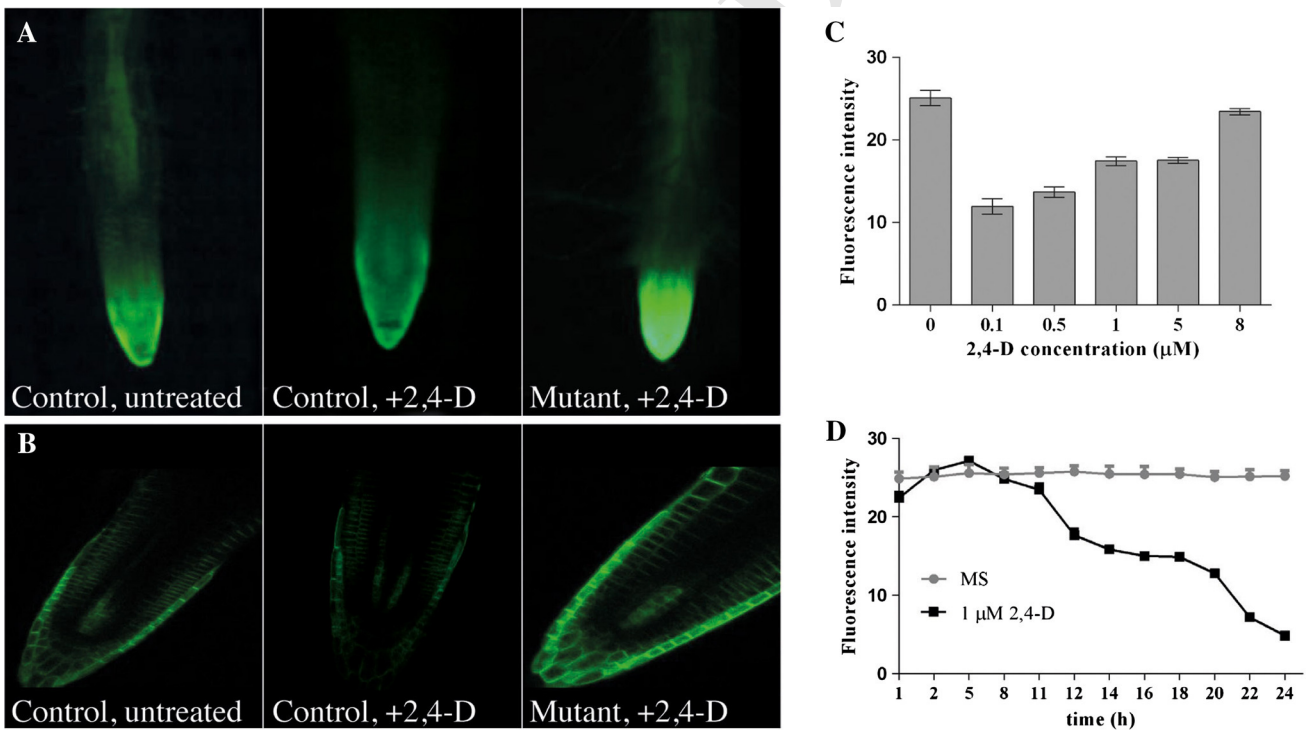

Fig. 1 Optimization of the screen conditions to isolate the *ade* mutants. The *PIN2*::*PIN2:GFP AUX1*::*AUX1:YFP aux1 pin2* EMS mutant population was screened for maintenance of the PIN2 or AUX1 fluorescence signal after 2,4-D treatments (**a**, **b**). Long treatment (20 h) with 2,4-D (1 μM) increases turnover of both fluorescent proteins in the control seedlings but not in the *ade* mutants. The primary screen was performed on a fluorescence stereomicroscope (**a**). Detailed analysis of the fluorescent signal was performed using a confocal microscope (**b**). Untreated control seedlings (*left panels*), treated control seedlings (*middle panels*), and an example of one *ade* mutant isolated in the screen after 2,4-D treatment (*right panels*). **c**–**d** Fluorescence signal intensity in control seedlings was measured after different 2,4-D concentrations after 12-h treatment (**c**) and after time points of 1uM 2,4-D treatment (**d**), as indicated. Seven roots per experiment were analysed. *Error bars* represent SD. See also Fig. S1

Journal : Large 344 Dispatch : 5-11-2015 Pages : 12
Article No. : 9553 LE TYPESET
MS Code : JPGR-15-0235 CP DISK

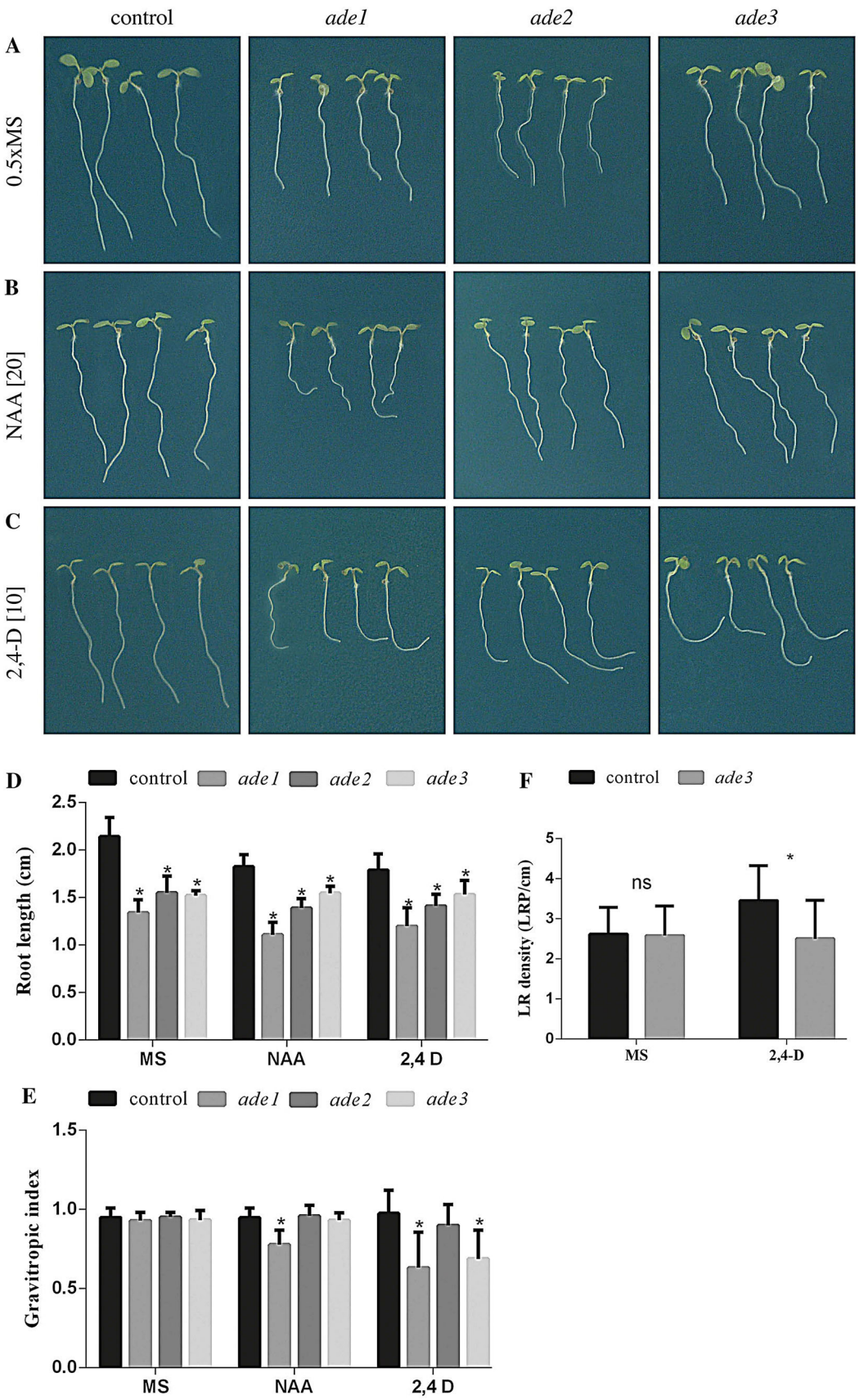

Journal : Large 344 Dispatch : 5-11-2015 Pages : 12
Article No. : 9553 LE TYPESET
MS Code : JPGR-15-0235 CP DISK

◀**Fig. 2** Seedling phenotypes of *ade* mutants grown under long-day growth conditions (**a**–**e**). The control line (*left panel* and *black columns*) and *ade1*, *ade2*, *ade3* mutants (*middle* and *right panels*, *grey columns*) were analysed for root phenotypes after germination and growth on auxin for 5 days [20 nM NAA (**b**), 10 nM 2,4-D (**c**), 0.5× MS is used as control (**a**)]. The mutant lines display a shorter primary root and are more sensitive to both auxins in terms of root length (**b**, **c**, **d**). ~~Shown is~~ one experiment of the three replicates, where 20 roots were analysed. *Error bars* represent SD. *Asterisk* indicates significant difference, $P < 0.05$. See also Figs. S2 and S5. **e** Gravitropic index was measured on roots of 5-day-old seedlings ($n = 20$ roots per experiment, one experiment presented out of three replicates). *Error bars* represent SD. *Asterisk* indicates significant difference, $P < 0.05$. See also Fig. S5. **f** Eight-day-old control line and *ade3* seedlings were grown on 0.5× MS and 0.5× MS supplemented with 10 nM 2,4-D and emerged lateral root (LR) density was quantified. *ade3* seedlings display reduced root length and a reduced number of emerged lateral roots as compared with the control line (*, $P < 0.05$). One representative experiment is shown, and 20 roots per mutant/treatment were analysed. *Error bars* represent SD. See also Figs. ~~S2,~~ S3 ~~and S5~~

roots (LRs) per cm of primary root. The gravitropic index was measured as the ratio of the vertical root length to the total root length. In all cases, plates were scanned using Epson Perfection V700 Photo Scanner and pictures were processed in Adobe Photoshop 7.0 to assemble the figures. ~~For analysis,~~ root length, hypocotyl length, gravitropic index and lateral root density were measured using the Java-based ImageJ application (National Institutes of Health; http://rsb.info.nih.gov/ij). Obtained values were processed in Excel software (version 11.3.3, Microsoft Corporation) and statistically analysed using GraphPad Prism 6.0 software (see detail below). For each experiment at least 20 seedlings per assay were measured in three independent replicates, giving the same statistically significant results. Results from one replicate are presented.

Cotyledon Vasculature Phenotype Analysis

Twelve-day-old cotyledons of *ade1–ade3* mutant seedlings were used and compared with Col-0 and control seedlings to identify specific venation phenotypes. The cotyledons were treated with 70 % EtOH for 2 h and 100 % EtOH until the cotyledons became transparent, following clearing for 2 h and mounting of the slide in a chloral hydrate solution (chloral hydrate (Sigma)/glycerol/water, 8/1/3, w/v/v). The experiment was repeated three times. At least 30 cotyledons from each genotype were analysed.

Fluorescent Signal Intensity Measurements of PIN2:GFP and AUX1:YFP

Five-day-old seedlings of the control line and *ade1–ade3* mutant lines were treated with 20 µM NAA for 3 h and imaged as described above. For the global signal intensity measurements presented in Fig. 5, two optical sections were scanned, one at the root surface focused on the PIN2:GFP epidermal expression (ep.) and another in the transversal median section (m.). Signal intensities were measured globally using the area function of the ImageJ software. For detailed quantification of the subcellular PIN2:GFP signals, fluorescence intensities of the plasma membrane signal or intracellular signal were measured separately by the area function of the Image J software.

Statistical Analysis

For analyses presented in Figs. 2d–f, 3d, 4, 5c, d, 6e, S2, S3 and S5, statistical analyses were performed using GraphPad Prism 6.0 software. For root, hypocotyl length and gravitropic index, a two-way ANOVA followed by Tukey's multiple comparisons test was performed. For analysis of relative root length, statistical significance was examined by one-way ANOVA followed by Tukey's multiple comparisons test. For lateral root development and lateral root density, a two-way ANOVA followed by ~~Sidaks~~ multiple comparisons test was performed. For analysis of the cotyledon vascular pattern, a χ^2 test was performed.

Results and Discussion

Design of Genetic Screen for *ade* Mutants Defective in Auxin-Regulated PIN2 and AUX1 Plasma Membrane Stabilization

To gain additional insight into the mechanism of PIN2 or AUX1 protein degradation and their stabilization at the plasma membrane and to identify molecular components that regulate this process, we designed a forward genetic screen. We generated transgenic ~~an~~ ~~*Arabidopsis*~~ line expressing *PIN2* and *AUX1* genes, fused to green fluorescent protein (GFP) and yellow fluorescent protein (YFP), respectively, under their native promoters in their corresponding *pin2* (*eir1-1*) and *aux1* mutant lines. This *PIN2*::*PIN2:GFP*~~,~~ *AUX1*::*AUX1:YFP eir1 aux1* was mutagenized by ethyl methanesulfonate (EMS), and we screened for mutants that showed a resistance to synthetic auxin 2,4-dichlorophenoxyacetic acid (2,4-D) in terms of ~~the 2,4-D~~ effect on protein degradation. This synthetic auxin is a weak substrate for intercellular auxin transport by PIN auxin efflux carriers (Petrášek and others 2006) and AUX1 auxin influx carriers (Marchant and others 1999) and is shown to be more stable than IAA and NAA (Seifertová and others 2014). 2,4-D is also known to induce additional, indirect effects such as post-translational modification of actin by oxidation and *S*-nitrosylation (Rodríguez-Serrano and others 2014). Therefore, all initial effects

Journal : Large 344 | Dispatch : 5-11-2015 | Pages : 12
Article No. : 9553 | LE | TYPESET
MS Code : JPGR-15-0235 | CP | DISK

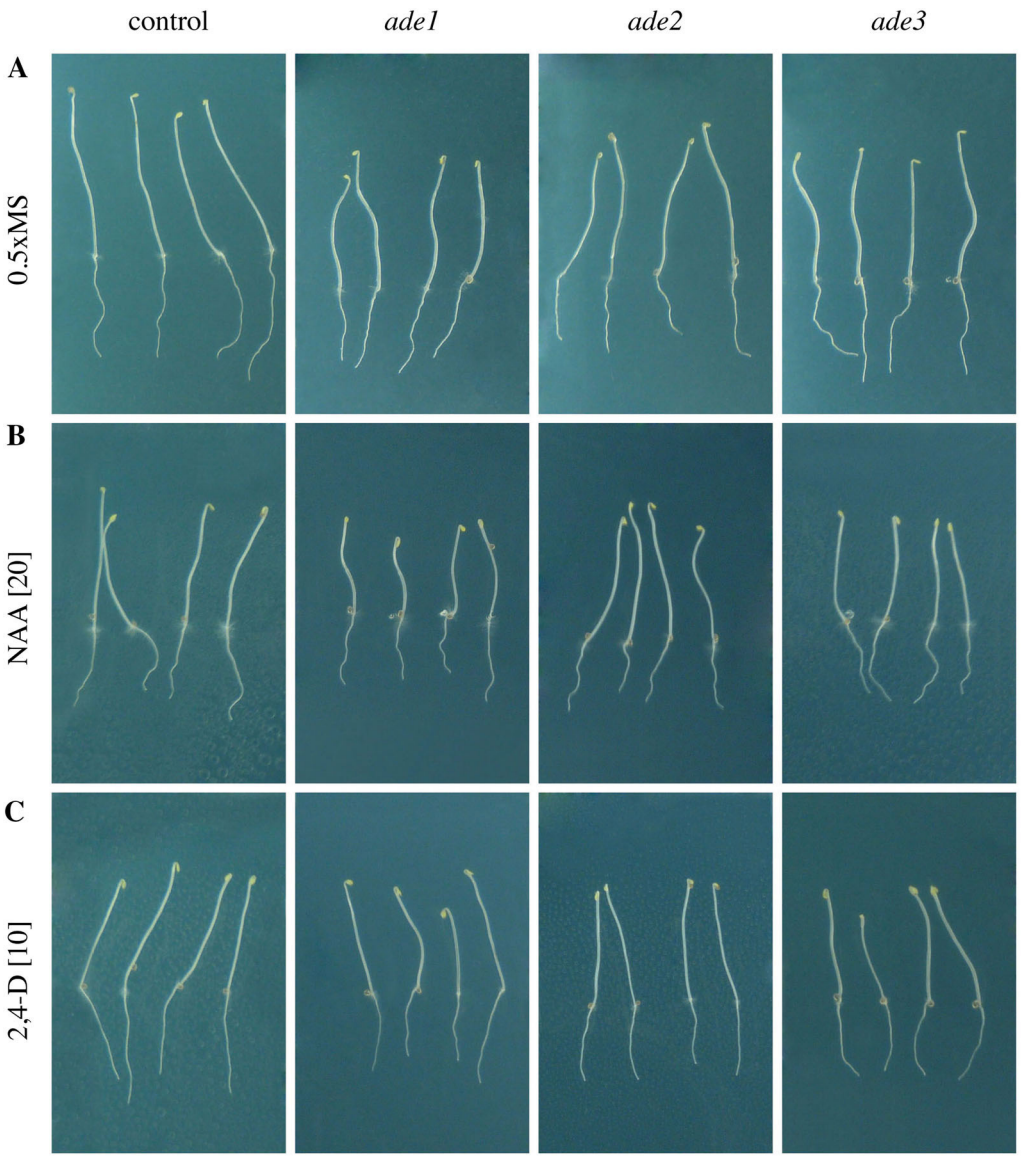

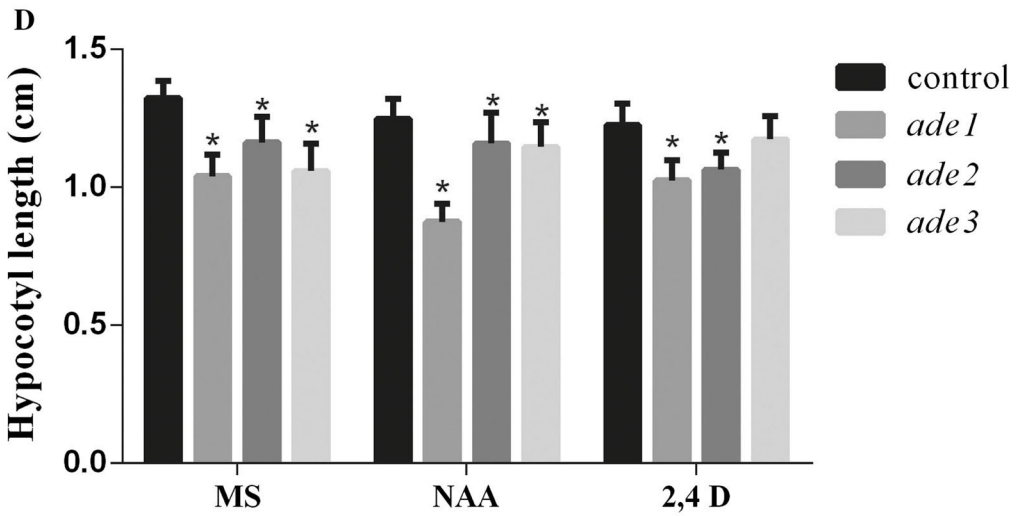

Journal : Large 344 Dispatch : 5-11-2015 Pages : 12
Article No. : 9553 LE TYPESET
MS Code : JPGR-15-0235 CP DISK

◀**Fig. 3** Phenotypes of etiolated *ade* mutants. Dark-grown control and *ade1–ade3* seedlings were germinated on 0.5× MS (**a**) or on 0.5× MS containing 20 nM NAA (**b**) or 10 nM 2,4-D (**c**) and were grown for 4 days, and length of their hypocotyls was measured (**d**). One representative experiment is shown, and 20 hypocotyls per mutant/treatment were analysed. *Error bars* represent SD. *Asterisk* indicates significant difference, $P < 0.05$. See also Fig. S5

observed using 2,4-D were later confirmed by treatments with other auxins.

Because this microscope-based forward genetic screen was time and work demanding, we designed one single screen to identify mutants defective in both AUX1- and PIN2 trafficking pathways. The prolonged 20-h treatment with 1 µM 2,4-D in non-mutagenized *PIN2*::*PIN2:GFP AUX1*::*AUX1:YFP eir1 aux1* seedlings (later referred ~~to~~ as control) increases turnover of both AUX1 and PIN2 proteins as visualized by the reduction of their fluorescence intensity at the plasma membrane (Fig. 1a, b). During long auxin treatments, we expected that 2,4-D would be best suited to "flood" all root cells more uniformly by auxin. To optimize the screening conditions, we tested different durations and concentrations of the 2,4-D treatment. Five-day-old control seedlings were treated for 12 h with different 2,4-D concentrations or with 1 µM 2,4-D for different durations and compared with untreated ~~(0.5× MS medium)~~ control seedlings in terms of global fluorescence intensity (Fig. 1c, d). We chose screening conditions as 1 µM 2,4-D for 20 h on solid medium, as it was experimentally better time versus concentration conditions to perform the screen, taking into account any possible degradation of auxin ~~contained~~ in the growth medium when stored. About 61–000 M2 seedling progenies of approximately 1500 M1 plants were grown for 4 days on 0.5× MS medium and transferred on new plates with 0.5× MS supplemented with 1 µM 2,4-D (for 20 h) and screened under a fluorescence stereomicroscope. After re-screening of the progeny of the 27 selected mutant candidates, 12 mutants were confirmed to show consistent and reliable elevated fluorescence signals either for PIN2:GFP or for AUX1:YFP (Fig. S1B–M). These are designated as *ade* mutants. Here we present the detailed characterization of *ade1* to *ade3* (Fig. S1K–M) including characterization of their morphological phenotypes.

Growth Phenotypes of *ade* Mutants

We outcrossed *ade* mutant lines into the control background and analysed homozygous lines for their phenotypes. Adult *ade1–ade3* displayed smaller stature and *ade3* showed early flowering (Fig. S1N). The *ade1–ade3* mutant seedlings have shorter roots when grown on 0.5× MS medium (Fig. 2a, d, Fig. S5). Only *ade2* and *ade3* lines also showed a decreased sensitivity to NAA and 2,4-D effect on root growth (Fig. 2b–d, Figs. S2, S5). When vertically grown on 2,4-D and to a lesser extend in NAA for *ade1*, the mutant roots had a tendency to deviate from normal vertical growth (Fig. 2c, e, Fig. S5). In addition, the *ade3* mutant line showed resistance to auxin in terms of

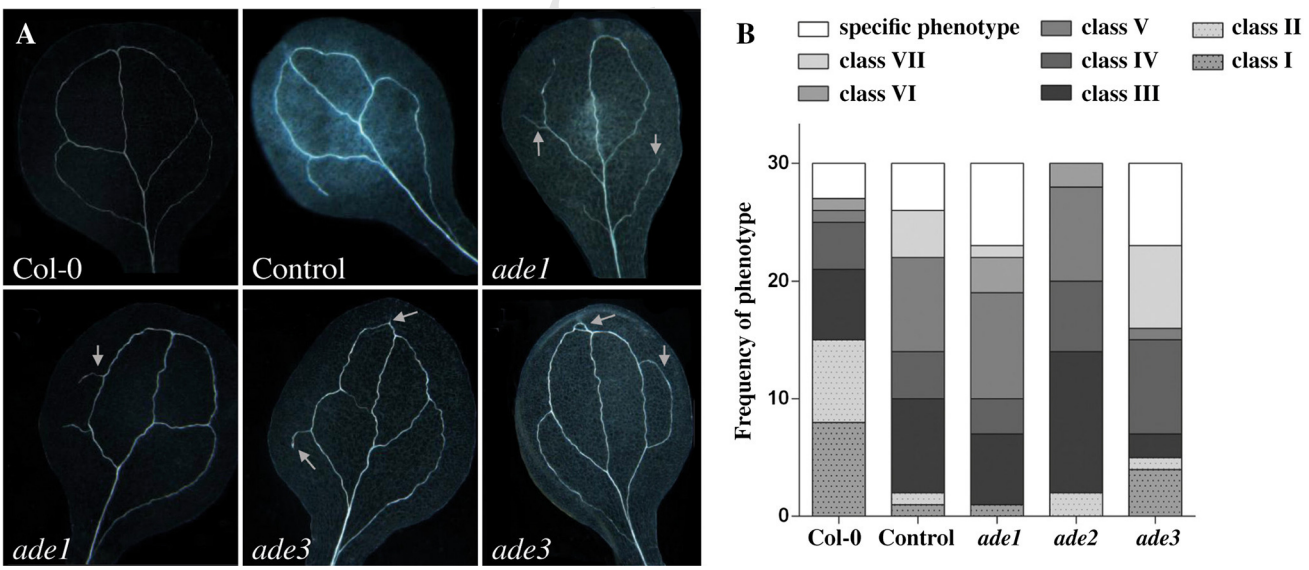

Fig. 4 Vasculature phenotypes of *ade* mutants. Twelve-day-old Col-0, control and *ade1*, *ade2*, *ade3* mutant seedlings were germinated on 0.5× MS medium. Cotyledon vasculature phenotypes were categorized (class I–VII, see for details Supplemental Fig. S4). Aberrant phenotypes (unusually disconnected or defective veins) were pooled in the "specific phenotype" category and shown in (**a**). A *graph* displays the distribution in the different categories of the vascular pattern in cotyledons (**b**). Thirty cotyledons per line were analysed. χ^2 analysis shows that *ade1* and *ade3* have a significantly more cotyledons categorized as "specific phenotype" than the three other analysed lines. See also Fig. S4

Journal : Large 344 | Dispatch : 5-11-2015 | Pages : 12
Article No. : 9553 | LE | TYPESET
MS Code : JPGR-15-0235 | CP | DISK

lateral root formation (Fig. 2f, Figs. S3, S5). Next we tested growth of *ade* mutants in dark conditions. *ade* mutant lines displayed shorter hypocotyls as compared with control seedlings (Fig. 3, Fig. S5). The mutant line *ade1* showed increased sensitivity to NAA treatment and *ade1* and *ade2* showed a decreased sensitivity to 2,4-D in terms of etiolated hypocotyl lengths (Fig. 3d, Fig. S5). These observations show that *ade* mutants originally identified as being defective in auxin-mediated protein turnover also showed a number of developmental defects.

Vascular Venation Pattern Defects in *ade* Mutants

The vascular system is constructed as a complex network pattern called venation. The formation of this vein pattern has been widely studied as a paradigm of tissue pattern formation in plants and is known to be strongly dependent on auxin transport (Koizumi and others 2005; Scarpella and others 2006; Zhang and others 2011). Therefore, we analysed vascular tissue formation in *ade1*, *ade2* and *ade3* mutants. Twelve-day-old cotyledons were used and compared with Col-0 and the control seedlings to identify specific venation phenotypes. The vascular venation pattern was classified into seven individual classes depending on the different type of defects ranging from freely ending, disconnected veins, different numbers and shapes of closed loops to "specific" phenotypes that were typical for different mutants and hardly occurred in control seedlings (Fig. S4). Already the control line showed a slightly altered vasculature pattern as compared with Col-0, presumably due to the background *eir1* and *aux1* mutations (Fig. 4a, b). Clear vascular pattern defects characterized by frequent free ends and disconnected loops were observed more predominantly in *ade1* and *ade3* mutant cotyledons. This shows that *ade1* and *ade3* but not *ade2* mutants are defective in vascular pattern formation—a typical auxin and auxin transport-mediated process.

PIN2:GFP and AUX1:YFP Signal Intensity in *ade* Mutants

ade mutants were isolated based on their increased PIN2:GFP and AUX1:YFP signal intensities in roots after prolonged treatment with auxin as compared with the control situation that led to a pronounced reduction of the fluorescent signal of both proteins. The evaluation by a fluorescence stereomicroscope allowed only for a quick but rough estimation of the signal intensities, and for more detailed examination of PIN2:GFP and AUX1:YFP signals, we used a confocal microscope. We examined 5-day-old control and *ade* mutant seedlings for global accumulation of PIN2:GFP (blue) and AUX1:YFP (green) signal after 1 μM 2.4-D treatment for 20 h. The fluorescence measurements of the PIN2:GFP and AUX1:YFP signal in surface (ep) and at the median (m) optical sections revealed an increased fluorescent signal intensity with and without auxin treatment in the mutant roots as compared with the control roots (Fig. 5). Notably, the PIN2-GFP signal in all 3 *ade* mutants was completely insensitive to the 2,4-D treatment (Fig. 5d). These results show that *ade* mutants have defects in auxin-dependent protein removal from the plasma membrane and in particular for PIN2. 2,4-D and other auxins are known to promote transcription of *PIN2* (Vieten and others 2005). The fact that we see a decreased intensity of the fluorescence signal of plasma membrane localized-PIN2 and AUX1 after 2,4-D treatments indicates that this auxin effect is unlikely to be transcriptionally dependent.

Auxin Effect in PIN2:GFP Signal Intensity

Auxin and dark conditions have been shown to promote PIN2 translocation to the vacuole for degradation and that this process requires treatment with synthetic auxin NAA (Baster and others 2013; Laxmi and others 2008). Therefore, we tested the effect of the NAA treatment both in light and dark conditions on PIN2:GFP localization as measured as a ratio of signal intensity at the plasma membrane versus signal intensity inside the cell. All *ade* mutants have a stronger PIN2:GFP signal at the plasma membrane as compared with the control and showed a down-regulation of the plasma membrane signal and a relative increase of the intracellular signals after transition of seedlings to the dark (Fig. 6). In light-grown *ade1* seedlings, PIN2:GFP strongly accumulated in the cell in unidentified cellular compartment in response to 3 h of 20 μM NAA treatment (higher fluorescence intensity of internal signal) and similarly after transfer to the dark (Fig. 6c, d). In contrast, *ade2* seedlings showed a much less intracellular signal accumulation in response to auxin both in light or dark conditions and *ade3* seedlings showed normal response in light but resistance to auxin treatment in dark conditions.

These data confirm that *ade* mutants have defects in AQ1 removal of PIN2 proteins from the plasma membrane and the different observations in different *ade* mutants indicate that these mutants are defective in different aspects of protein trafficking and presumably degradation machinery.

Conclusion

Regulated degradation of plasma membrane proteins in vacuoles is a fundamental cellular process that is involved in the regulation of not only cellular homeostasis but also many aspects related to physiology and development of

Journal : Large 344 Dispatch : 5-11-2015 Pages : 12
Article No. : 9553 LE TYPESET
MS Code : JPGR-15-0235 CP DISK

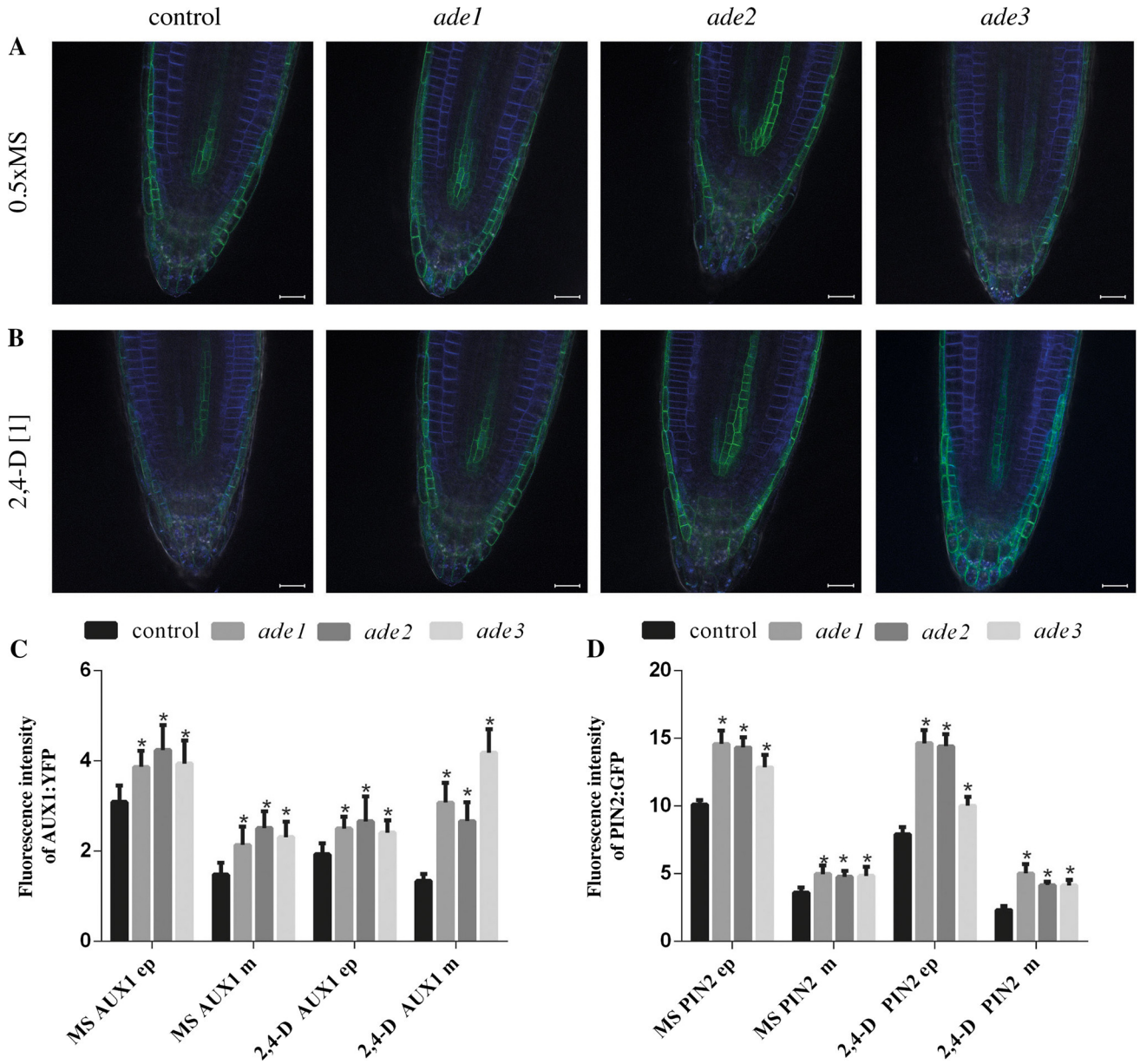

Fig. 5 Fluorescence intensity of PIN2::PIN2:GFP and AUX1::-AUX1:YFP in *ade* mutants after auxin treatment. Localization of PIN2:GFP (*blue*) and AUX1:YFP (*green*) in 5-day-old control line (*left panel*) and *ade1-3* mutants grown on 0.5× MS (**a**) or after a 20-h treatment with 1 µM 2,4-D (**b**). (**c**, **d**) The fluorescence intensity was measured in two confocal sections, one focused on the surface of the root [epidermal (ep)] and another as middle transversal (m). The PIN2:GFP signal was quantified in both sections in epidermal and cortical cells, and AUX1:YFP in epidermal cells (surface section, ep) and lateral root cap, epidermal cells, columella and stele (transversal section, m). In the control root, the fluorescence intensity decreased upon auxin treatment in all cases but not in *ade* roots. One representative experiment is displayed, and 20 roots per treatment per genotype were analysed. *Error bars* represent SD. *Asterisk* indicates significant difference, ($P < 0.05$). *Scale bar* represents 20 µm

multicellular organisms. In particular, vacuolar trafficking and degradation of the PIN auxin transport components and feedback regulation by auxin itself have been demonstrated to play a role during developmental processes such as root gravitropism (Abas and others 2006; Baster and others 2013; Kleine-Vehn and others 2008). Also the regulation of PIN degradation by other signals such as light (Laxmi and others 2008) and plant hormones cytokinin (Marhavy and others 2011) and gibberellic acid (Löfke and others 2013) plays an important developmental role.

To gain additional molecular insight into the regulation of PIN degradation by auxin, we designed a forward genetic screen to identify mutants defective in these processes. The screen is based on the EMS-mutagenized

Journal : Large 344 Dispatch : 5-11-2015 Pages : 12
Article No. : 9553 LE TYPESET
MS Code : JPGR-15-0235 CP DISK

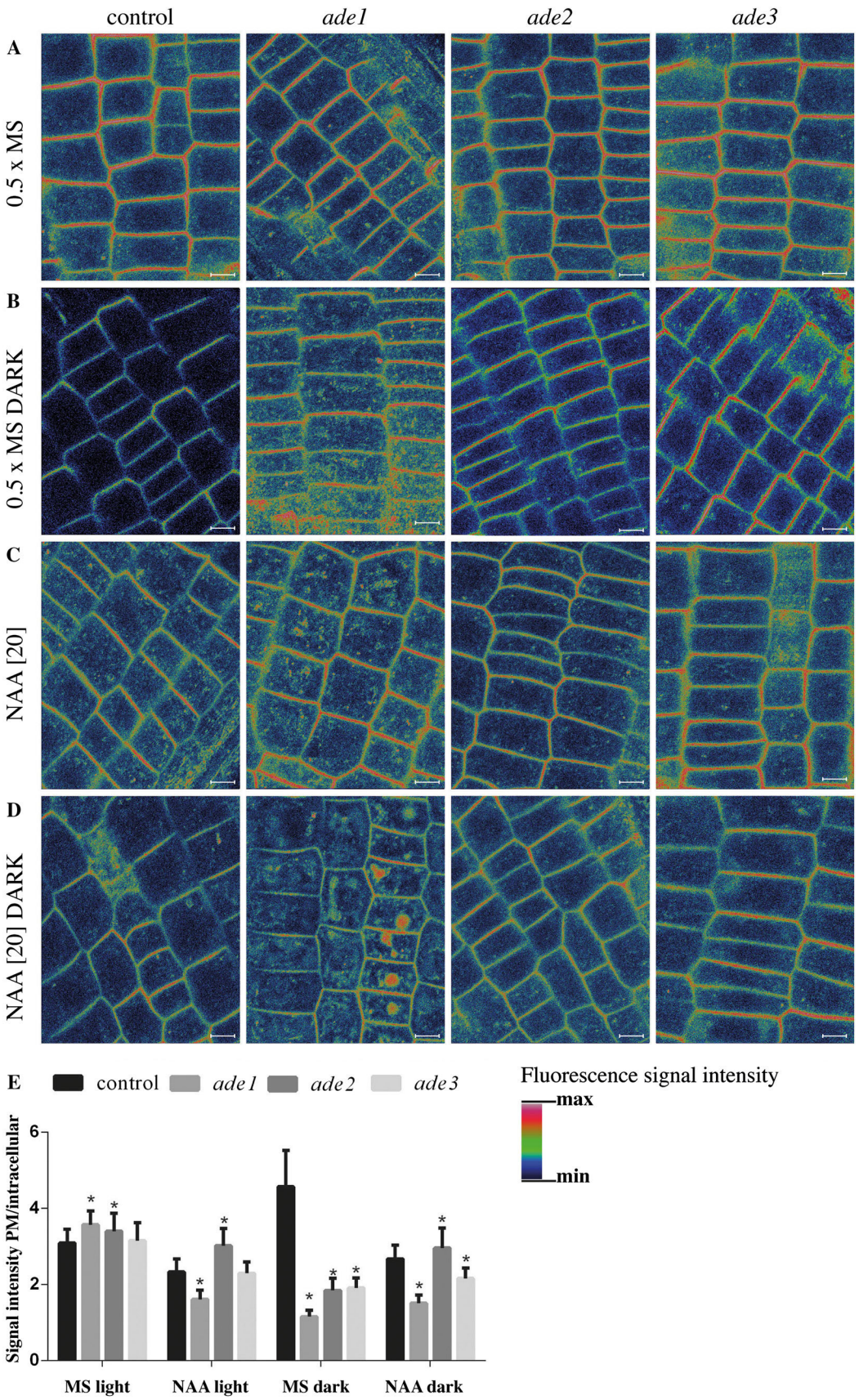

Journal : Large 344 Dispatch : 5-11-2015 Pages : 12
Article No. : 9553 LE TYPESET
MS Code : JPGR-15-0235 CP DISK

◀**Fig. 6** Auxin-mediated subcellular internalization of PIN2:GFP signal in root epidermal cells. Five-day-old control line and *ade1*, *ade2* and *ade3* mutant seedlings were germinated and grown on 0.5× MS medium under long-day growth conditions and treated without (**a**) or with 20 μM NAA for 3 h (**c**), or transferred to darkness without (**b**) or with 20 μM NAA for 3 h (**d**). **a**–**d** Confocal images of the PIN2:GFP fluorescence signal in root epidermal cells. The fluorescence signal is displayed as a *red–green–blue* false colour fluorescence intensity gradient. **e** The fluorescence PIN2:GFP signal intensity was measured at the plasma membrane and intracellularly, and the signal intensity ratio was plotted. The *graph* shows that the PIN2:GFP signal ratio in the control line was enhanced by dark treatment and in both conditions (light and dark) reduced by auxin treatment. The signal intensity ratio in *ade* dark-treated is greatly reduced. Ten roots were analysed for each assay, and signal intensity was measured in ten cells per root ($n = 100$ cells per treatment/genotype). *Error bars* represent SD. *Asterisk* indicates significant difference, $P < 0.05$. *Scale bar* represents 5 μm

population expressing PIN2:GFP and AUX1:YFP markers under their own promoters and in both mutant backgrounds. The conditions were optimized allowing for efficient long-term auxin treatment and screening under a fluorescent stereomicroscope. The screen of 1500 M1 families yielded 12 *ade* mutants with defects in auxin-dependent plasma membrane protein removal. Three *ade* mutants (*ade1–ade3*) were characterized in more detail and after outcrossing showed different developmental defects in auxin-mediated developmental processes such as gravitropism, root response to auxin and vascular pattern formation. In general, the observed root growth phenotype in response to auxin is to some extent similar to what were observed in *tir1/afb* signalling mutants (Dharmasiri and others 2005). In addition, vascular defects are reminiscent of auxin transport defects (Koizumi and others 2005; Scarpella and others 2006; Zhang and others 2011). These *ade* mutants displayed different defects in plasma membrane AUX1 and PIN2 turnover and in auxin- or light-induced PIN2 intracellular trafficking.

Although the molecular nature of the *ade* mutations has yet to be discovered and remains the immediate experimental challenge, the identification and characterization of *ade1*, *ade2* and *ade3* mutants revealed that the designed mutant screening strategy is instrumental in identifying components of the auxin-dependent regulation of protein trafficking and degradation machinery.

Acknowledgments We thank Eva Huspekova and David John Hanley for kindly help in preparing this manuscript, and Klara Harmanova and Radka Holbova for technical help. This work was supported by the European Research Council (project ERC-2011-StG-20101109-PSDP); European Social Fund (CZ.1.07/2.3.00/20.0043) and the Czech Science Foundation GAČR (GA13-40637S) to JF. Work was realized in CEITEC – Central European Institute of Technology (CZ.1.05/1.1.00/02.0068). M.Z. was supported by Project Postdoc I (CZ.1.07/2.3.00/30.0009) co-financed by the European Social Fund and the state budget of the Czech Republic. H.S.R was supported by the SoMoProII program (3SGA5602), co-financed by the South-Moravian Region and the EU (FP/2007-2013, Grant Agreement No. 291782).

References

Abas L, Benjamins R, Malenica N, Paciorek T, Wiśniewska J, Moulinier-Anzola JC, Sieberer T, Friml J, Luschnig C (2006) Intracellular trafficking and proteolysis of the *Arabidopsis* auxin-efflux facilitator PIN2 are involved in root gravitropism. Nat Cell Biol 8:249–256

Adamowski M, Friml J (2015) PIN-dependent auxin transport: action, regulation, and evolution. Plant Cell 27:20–32

Baster P, Robert S, Kleine-Vehn J, Vanneste S, Kania U, Grunewald W, De Rybel B, Beeckman T, Friml J (2013) SCF(TIR1/AFB)-auxin signalling regulates PIN vacuolar trafficking and auxin fluxes during root gravitropism. EMBO J 32:260–274

Bennett MJ, Marchant A, Green HG, May ST, Ward SP, Millner PA, Walker AR, Schulz B, Feldmann KA (1996) *Arabidopsis* AUX1 gene: a permease-like regulator of root gravitropism. Science 273:948–950

Dharmasiri N, Dharmasiri S, Weijers D, Lechner E, Yamada M, Hobbie L, Ehrismann SJ, Jürgens G, Estelle M (2005) plant development is regulated by a family of auxin receptor F box proteins. Dev Cell 9:109–119

Feraru E, Friml J (2008) PIN polar targeting. Plant Physiol 147:1553–1559

Feraru E, Paciorek T, Feraru MI, Zwiewka M, De Groodt R, De Rycke R, Kleine-Vehn J, Friml J (2010) The AP-3 β adaptin mediates the biogenesis and function of lytic vacuoles in *Arabidopsis*. Plant Cell 22:2812–2824

Kleine-Vehn J, Dhonukshe P, Sauer M, Brewer PB, Wiśniewska J, Paciorek T, Benková E, Friml J (2008) ARF GEF-dependent transcytosis and polar delivery of PIN auxin carriers in *Arabidopsis*. Curr Biol 18:526–531

Koizumi K, Naramoto S, Sawa S, Yahara N, Ueda T, Nakano A, Sugiyama M, Fukuda H (2005) VAN3 ARFGAP-mediated vesicle transport is involved in leaf vascular network formation. Development 132:1699–1711

Laxmi A, Pan J, Morsy M, Chen R (2008) light plays an essential role in intracellular distribution of auxin efflux carrier PIN2 in *Arabidopsis thaliana*. PLoS ONE 3:1510

Löfke C, Zwiewka M, Heilmann I, Van Montagu MCE, Teichmann T, Friml J (2013) Asymmetric gibberellin signaling regulates vacuolar trafficking of PIN auxin transporters during root gravitropism. PNAS 110:3627–3632

Luschnig C, Gaxiola RA, Grisafi P, Fink GR (1998) EIR1, a root-specific protein involved in auxin transport, is required for gravitropism in *Arabidopsis thaliana*. Genes Dev 14:2175–2187

Malamy JE, Benfey PN (1997) Organization and cell differentiation in lateral roots of *Arabidopsis thaliana*. Development 124:33–44

Marchant A, Kargul J, May ST, Muller P, Delbarre A, Perrot-Rechenmann C, Bennett MJ (1999) AUX1 regulates root gravitropism in *Arabidopsis* by facilitating auxin uptake within root apical tissues. EMBO J 18:2066–2073

Marhavy P, Bielach A, Abas L, Abuzeineh A, Duclercq J, Tanaka H, Parezová M, Petrášek J, Friml J, Kleine-Vehn J, Benková E (2011) Cytokinin modulates endocytic trafficking of PIN1 auxin efflux carrier to control plant organogenesis. Dev Cell 21:796–804

Nodzynski T, Feraru MI, Hirsch S, De Rycke R, Niculaes C, Boerjan W, Van Leene J, De Jaeger G, Vanneste S, Friml J (2013) Retromer subunits VPS35A and VPS29 mediate prevacuolar

Journal : Large 344 | Dispatch : 5-11-2015 | Pages : 12
Article No. : 9553 | ☐ LE | ☐ TYPESET
MS Code : JPGR-15-0235 | ☑ CP | ☑ DISK

compartment (PVC) function in *Arabidopsis*. Mol Plant 6:1849–1862

Paciorek T, Zažímalová E, Ruthardt N, Petrášek J, Stierhof YD, Kleine-Vehn J, Morris DA, Emans N, Jürgens G, Geldner N, Friml J (2005) Auxin inhibits endocytosis and promotes its own efflux from cells. Nature 435:1251–1256

Petrášek J, Mravec J, Bouchard R et al (2006) PIN proteins perform a rate-limiting function in cellular auxin efflux. Science 312:914–918

Robert S, Kleine-Vehn J, Barbez E et al (2010) ABP1 mediates auxin inhibition of clathrin-dependent endocytosis in *Arabidopsis*. Cell 143:111–121

Rodríguez-Serrano M, Pazmiño DM, Sparkes I, Rochetti A, Hawes C, Romero-Puertas MC, Sandalio LM (2014) 2,4-dichlorophenoxyacetic acid promotes *S*-nitrosylation and oxidation of actin affecting cytoskeleton and peroxisomal dynamics. J Exp Bot 17:4783–4793

Sauer M, Balla J, Luschnig C, Wiśniewska J, Reinöhl V, Friml J, Benková E (2006) Canalization of auxin flow by Aux/IAA-ARF-dependentfeedback regulation of PIN polarity. Genes Dev 20:2902–2911

Scarpella E, Marcos D, Friml J, Berleth T (2006) Control of leaf vascular patterning by polar auxin transport. Genes Dev 20:1015–1027

Seifertová D, Skupa P, Rychtář J et al (2014) Characterization of transmembrane auxin transport in *Arabidopsis* suspension-cultured cells. J Plant Physiol 171:429–437

Sieberer T, Seifert GJ, Hauser MT, Grisafi P, Fink GR, Luschnig C (2000) Post-transcriptional control of the *Arabidopsis* auxin efflux carrier EIR1 requires AXR1. Curr Biol 10:1595–1598

Swarup R, Friml J, Marchant A, Ljung K, Sandberg G, Palme K, Bennett M (2001) Localization of the auxin permease AUX1 suggests two functionally distinct hormone transport pathways operate in the *Arabidopsis* root apex. Genes Dev 15:2648–2653

Tanaka H, Kitakura S, De Rycke R, De Groodt R, Friml J (2009) Fluorescence imaging-based screen identifies ARF GEF component of early endosomal trafficking. Curr Biol 19:391–397

Tanaka H, Kitakura S, Rakusova H, Uemura T, Feraru MI, De Rycke R, Robert S, Kakimoto T, Friml J (2013) Cell polarity and patterning by PIN trafficking through early endosomal compartments in *Arabidopsis thaliana*. PLoS Genet 9:e1003540

Tanaka H, Nodzynski T, Kitakura S, Feraru MI, Sasabe M, Ishikawa T, Kleine-Vehn J, Kakimoto T, Friml J (2014) BEX1/ARF1A1C is required for BFA-sensitive recycling of PIN auxin transporters and auxin-mediated development in *Arabidopsis*. Plant Cell Physiol 55:737–749

Vieten A, Vanneste S, Wiśniewska J, Benková E, Benjamins R, Beeckman T, Luschnig C, Friml J (2005) Functional redundancy of PIN proteins is accompanied by auxin-dependent cross-regulation of PIN expression. Development 132:4521–4531

Wiśniewska J, Xu J, Seifertová D, Brewer PB, Ruzicka K, Blilou I, Rouquié D, Benková E, Scheres B, Friml J (2006) Polar PIN localization directs auxin flow in plants. Science 312:858–860

Xu J, Scheres B (2005) Dissection of *Arabidopsis* ADP-RIBOSYLATION FACTOR **1** function in epidermal cell polarity. Plant Cell 17:525–536

Zhang J, Vanneste S, Brewer PB et al (2011) Inositol trisphosphate-induced Ca2+ signaling modulates auxin transport and PIN polarity. Dev Cell 20:855–866

Zwiewka M, Feraru E, Möller B, Hwang I, Feraru MI, Kleine-Vehn J, Weijers D, Friml J (2011) The AP-3 adaptor complex is required for vacuolar function in *Arabidopsis*. Cell Res 21:1711–1722

Journal : **Large 344** Dispatch : **5-11-2015** Pages : **12**
Article No. : **9553** ☐ LE ☐ TYPESET
MS Code : **JPGR-15-0235** ☑ CP ☑ DISK